Evaluation of Multisensor Quantitative Precipitation Estimation in Russian River Basin

Delbert Willie[1]; Haonan Chen[2]; V. Chandrasekar[3]; Robert Cifelli[4]; Carroll Campbell[5]; David Reynolds[6]; Sergey Matrosov[7]; and Yu Zhang[8]

Abstract: An important goal of combining weather radar with rain gauge data is to provide reliable estimates of rainfall rate and accumulation and to further identify intense precipitation and issue flood warnings. Scanning radars provide the ability to observe precipitation over wider areas within shorter timeframes compared to rain gauges, leading to improved situational awareness and more accurate and reliable warnings of future precipitation and flooding events. The focus of this study is on evaluating the performance of the multi-radar multi-sensor (MRMS) system with and without the impact of a local gap filling radar. The challenge of using radar and rain gauges to provide accurate rainfall estimates in complex terrain is investigated. The area of interest is the Russian River basin north of San Francisco, CA, which lies within the National Oceanic and Atmospheric Administration (NOAA) Hydrometeorology Testbed (HMT). In this complex mountainous terrain, the challenge of obtaining reliable quantitative precipitation estimations (QPEs) is hindered by beam blockage and overshooting, as well as the enhancement of rainfall on the windward side of mountain ranges. The effectiveness of several local radars, which include four S-band National Weather Service (NWS) Weather Surveillance Radar–1988 Doppler (WSR-88DP) radars and a C-band gap filling TV station radar (i.e., KPIX), are considered for deriving QPE over this region. The precipitation estimation methodologies used the MRMS algorithms and an independent KPIX-only ($Z - R$) based QPE algorithm. In addition, a time series analysis is conducted in order to illustrate the radar-gauge rainfall difference caused by radar beam height. The sampling relative to precipitation vertical structure is also considered in regards to the depth of the precipitation and the height of the bright band. The quantitative evaluation of different QPE products is presented.
DOI: 10.1061/(ASCE)HE.1943-5584.0001422.

Introduction

The estimation of rainfall rate and accumulation is one of the important applications of weather sensing radars (Bringi and Chandrasekar 2001; Cifelli and Chandrasekar 2010; Chen and Chandrasekar 2015). However, in complex terrain like the Russian River basin (Fig. 1), it is a challenging task to obtain the best empirical $Z - R$ relation. In addition, the accuracy of rain rate estimates is contingent on additional factors such as radar calibration, vertical profile of reflectivity (VPR), beam blockages, bright bands, and anomalous propagation (Zhang et al. 2011a; Kitzmiller et al. 2011; Kitchen et al. 1994; Fulton et al. 1998; Cifelli et al. 2013; Willie et al. 2013). The Russian River basin is situated between the Mayacamas mountain range to the east and Coastal mountains to the west where low-level elevation radar coverage from national weather service (NWS) next generation weather radar (NEXRAD) over this area is not possible (Maddox et al. 2002). A gap filling non-NEXRAD radar (hereafter referred to as KPIX) that provides improved coverage over the basin is also considered for the purposes of quantitative precipitation estimation (QPE). KPIX is a C-band, single polarization radar owned and operated by a commercial broadcast station.

This case study has two goals. The first is to determine the best QPE in this region using the suite of products generated by the multi-radar multi-sensor (MRMS), also known as national mosaic & multi-sensor QPE (NMQ) algorithm package, which is developed by the National Severe Storms Laboratory (NSSL) (Zhang et al. 2011a). The second is to evaluate the contributions of KPIX radar to QPE in this region such that MRMS QPE products are evaluated over the Russian River basin using NEXRAD radar with and without KPIX, and then using KPIX only as input. The radar input combination is chosen to establish the relative impact of NEXRAD and gap-filling radars on QPE in this region. Rainfall events in this study consist of 27 days in 2013 and 2014 during the annual cool stratiform season. This type of rainfall is typical in this region and is a result from the atmospheric river conditions (Ralph et al. 2011). The rainfall accumulation periods include 1, 3, and 6 h, in order to both study the flash flooding impacts and allow for comparison with River Forecast Centers (RFC) QPE products. The QPE performance is evaluated with nine validation gauges.

Currently the NWS California Nevada River Forecast Center (CNRFC) does not use radar information to produce the mean areal

[1]Research Scientist, Colorado State Univ., 1373 Campus Delivery, Fort Collins, CO 80523 (corresponding author). E-mail: dwillie@engr.colostate.edu
[2]Research Assistant, Colorado State Univ., Fort Collins, CO 80523.
[3]University Distinguished Professor, Colorado State Univ., Fort Collins, CO 80523.
[4]Meteorologist, NOAA/Earth System Research Laboratory, Boulder, CO 80305.
[5]Electrical Engineer, Cooperative Institute for Research in Environmental Sciences, Univ. of Colorado Boulder, and NOAA/Earth System Research Laboratory, Boulder, CO 80305.
[6]Senior Research Meteorologist, Cooperative Institute for Research in Environmental Sciences, Univ. of Colorado Boulder, and NOAA/Earth System Research Laboratory, Boulder, CO 80305.
[7]Senior Research Scientist, Cooperative Institute for Research in Environmental Sciences, Univ. of Colorado Boulder, and NOAA/Earth System Research Laboratory, Boulder, CO 80305.
[8]Physical Scientist, Office of Hydrologic Development, National Weather Service, 1325 East-West Highway, Silver Spring, MD 20910.

Note. This manuscript was submitted on February 9, 2015; approved on April 13, 2016; published online on July 13, 2016. Discussion period open until December 13, 2016; separate discussions must be submitted for individual papers. This paper is part of the ***Journal of Hydrologic Engineering***, © ASCE, ISSN 1084-0699.

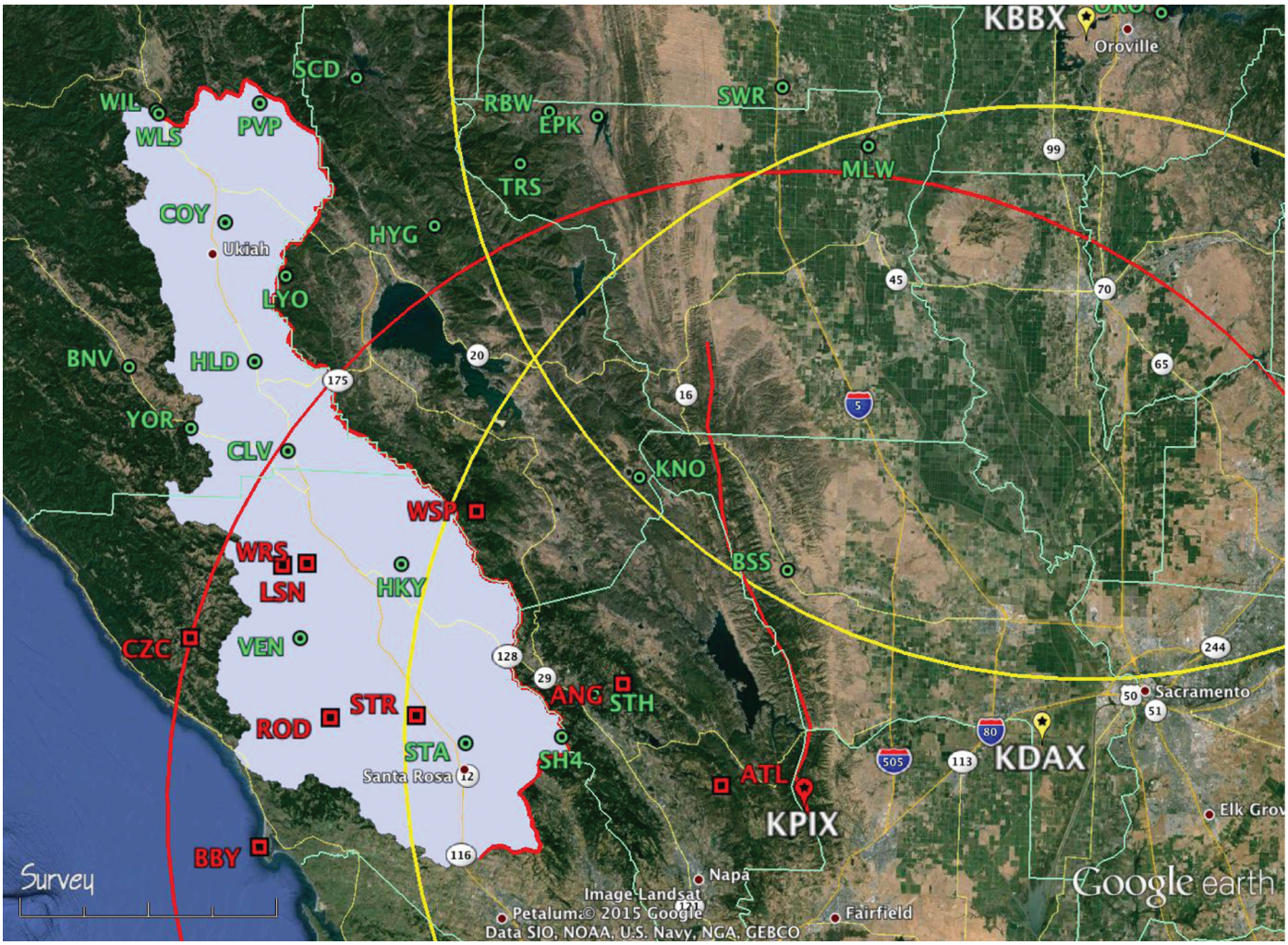

Fig. 1. (Color) Study domain with 100 km radar range rings (NEXRAD: yellow, KPIX: red); analysis and validation gauges designated by green circles and red squares, respectively (Image Landsat, (c) 2015 Google, Data SIO, NOAA, U.S. Navy, NGA, and GEBCO)

precipitation that is used to drive the NWS River Forecast System (NWSRFS) for the Russian River. It relies on rain gauge data and rainfall climatology [i.e., Parameter-elevation Regressions on Independent Slopes Model (PRISM)] in a procedure called Mountain Mapper (Schake et al. 2004). In this paper, the authors attempt to evaluate the benefits of a combined radar-gauge rainfall system to produce 6 h QPEs that can be input to NWSRFS. Most of the NWS RFCs east of the Rockies use radar information via the multi-sensor precipitation estimator (MPE) system. The hourly MPE QPE is ingested by the RFC's client NWS Weather Forecast Offices to further improve the flash flood monitoring and prediction (FFMP) system, which uses gridded high resolution QPE (1km by 1km by 5 min) to produce flash flood forecasting (Kitzmiller et al. 2011). This gridding improves both the hourly and 6 h QPEs over current gauge-only methods in the western United States and provides positive impacts on main-stem river flood forecasts, as well as local flash flood forecasts.

Quantitative Precipitation Estimation Packages and Products

Offline versions of both MRMS and MPE were set up at the NOAA Earth System Research Laboratory (ESRL) for retrospective QPE analyses. Both systems have been described extensively in the literature (for MRMS, see Zhang et al. 2011a; for MPE, see Lawrence et al. 2003; Seo et al. 2010). Nevertheless, MPE data are only available for a subset of the rain events in this study. When available, MPE is used as a proxy for Mountain Mapper because the ESRL version of MRMS does not include Mountain Mapper and the MPE gauge-only QPE (i.e., GMOSAIC) uses PRISM climatology in a similar fashion to the Mountain Mapper technique.

Description of MRMS System

In this section, the salient features of MRMS with regard to the present analysis are described. For details, the reader is referred to Zhang et al. (2011a). MRMS is a distributed computing architecture with four major processing components. These system sections consist of (1) single radar processing, (2) two and three dimensional radar mosaics, (3) next-generation QPE (Vasiloff et al. 2007), and (4) evaluation. System input data sources comprise of NEXRAD level-II data, rapid update cycle (RUC) model-based hourly rainfall analyses (Benjamin et al. 2004), lightning data, hydrometeorological automated data system (HADS), and regional rain gauge networks.

MRMS Products of Interest: Gauge-Only, Radar-Only, Radar VPR, and Gauge Correction

Once the precipitation type has been identified and the 2D hybrid scan reflectivity fields are mosaicked using a weighting algorithm

to account for both distance and height of the radar beams from different radars. QPE is then derived based on the methodologies described in Zhang et al. (2011a). The mosaicked field has a spatial resolution of 1 km by 1 km and an update time of 2.5 min. The QPE fields in MRMS include radar-only, radar-only with VPR correction, radar with VPR and gauge correction, and gauge-only QPE. MRMS produces these rainfall products based on the availability of input data. 1 and 3 h rainfall accumulations are calculated every 5 min, and the 6, 12, 24, 48, and 72 h rainfall accumulations are aggregated from 1 h accumulations. QPE results are calculated from radar reflectivity resulting from all quality control mechanisms, mosaicking technique, and the appropriate identification of precipitation type (Zhang et al. 2011a). The implementation of dual polarization rainfall algorithms within MRMS is still under development. Therefore the MRMS radar-only QPE is only based on the measured reflectivity, whereas the radar-only with VPR correction computes QPE using the corrected reflectivity and the default $Z - R$ relation for stratiform rain (i.e., $Z = 200R^{1.6}$). In this paper, the default $Z - R$ relation is replaced with the $Z - R$ relation given by Martner et al. (2008) and Zhang et al. (2012), which is developed particularly for nonbright band rain in northern California coastal mountain regions

$$Z = 44R^{1.91} \tag{1}$$

where Z is in $\mathrm{mm^6\,m^{-3}}$; and R is in $\mathrm{mm\,h^{-1}}$.

One of the major challenges encountered with radar rainfall estimation is attempting to derive QPE from radar reflectivity observations for areas where such observations are enhanced by melting ice particles to form the so-called bright band. In order for MRMS to have an efficient real-time application for bright band correction, a two-step approach is used to determine the VPR. The first step is to calculate the mean volume scan VPR using the method described in Vignal et al. (2000). Then, model an idealized VPR from the mean values as described in Zhang et al. (2008).

In MRMS, gauge-based radar rainfall correction is conducted based on the technique described in Ware (2005).

Data Set

In this paper, the data set stems from a combination of operational radar and gauge observations as well as data from the NOAA Hydrometeorology Testbed (HMT) in the Russian River basin north of San Francisco, CA. Twenty-seven days of rainfall data collected during the months of March, November, and December of 2012 and February of 2014 are considered, including the following rain events: March 14–16, March 27–28, November 17–21, November 28–30, December 1–6, December 20–23 of 2012, and February 7–9 of 2014. Dominant precipitation in this region during the cool season is stratiform rain (Matrosov et al. 2014) with radar bright band heights ranging from about 1.5 to 2.5 km above the mean sea level (MSL) as observed by the NOAA S-band profiler located at Santa Rosa, CA (STR–Fig. 1). Bright band heights for each day are shown in Table 1.

MRMS rain gauge input consists of 57 gauges (hereafter referred to as analysis gauges) that are a combination of California Data Exchange Center (CDEC) gauges, NWS HADS gauges, and the NOAA HMT gauges (green dots in Fig. 1). Prior to MRMS gauge processing, a QC algorithm is performed on the analysis gauges to remove possible outliers or uncertain gauge values (Zhang et al. 2011b). Validation gauges (red squares in Fig. 1), which are independent from the analysis gauges, are comprised of nine gauges from the CDEC, HADS, and HMT gauge sets. For the validation gauge selection, an attempt has been made to achieve a balance of high and low elevations and a range of distances to the KPIX radar. The gauge elevations (indicated by the blue bars) relative to the radar beam heights and beam widths are illustrated in Fig. 2. The QC process for the validation gauges comprised of cross correlating with each other and visually identifying and removing outlying gauge values.

Table 1. Bright Band (BB) Heights Observed by the NOAA S-Band Profiler Located Near Santa Rosa, CA (STR) Located (32.8515°, −122.8022°) at An Elevation of 32 m MSL

Date (YYYY/MM/DD)	BB height (m)
2012/03/14	2,000
2012/03/15	2,000
2012/03/16	2,000
2012/03/27	1,500
2012/03/28	1,500
2012/11/16	NA
2012/11/17	2,250
2012/11/18	2,000
2012/11/19	NA
2012/11/20	2,250
2012/11/21	2,250
2012/11/28	2,000
2012/11/29	2,000
2012/11/30	2,000
2012/12/01	NA
2012/12/02	2,250
2012/12/03	NA
2012/12/04	2,500
2012/12/05	2,500
2012/12/06	NA
2012/12/20	2,000
2012/12/21	2,000
2012/12/22	1,250
2012/12/23	1,500
2014/02/07	1,500
2014/02/08	2,500
2014/02/09	2,250

Note: NA indicates that data were not available for this date.

MRMS radar input data comprises the surrounding NEXRAD radars (i.e., KMUX, KDAX, KBHX, and KBBX) with the addition of the TV station radar (i.e., KPIX) (Fig. 1). The NEXRAD radars are conducting volume scans in precipitation mode and delivering observations updated every five to six minutes, whereas the KPIX radar was primarily operated in a single scan mode with an update every minute. To gain insight into KPIX radar calibration, a common volume between the NEXRAD KDAX radar beam at 1.38° elevation and KPIX radar beam at 0.5° elevation at a range of 56 km from both radars was selected to cross compare reflectivity observations. The mean difference in reflectivity was found to be 2.2 dBZ for measurements greater than 15 dBZ for a six-hour rain event occurring on March 17, 2012, and thus indicates that KPIX is slightly underestimating compared with KDAX radar.

In addition, an examination of beam blockage of the two nearest radars (KDAX and KPIX) over the validation gauges is presented. KDAX provides the lowest NEXRAD unobstructed scan over the Russian River valley at 1.45° elevation for average atmospheric propagation conditions. Fig. 3 shows mountain profiles of beam blockage as seen from KDAX and KPIX in the direction of the Russian River basin, in Fig. 3(a). The red squares are the validation gauge locations, and the yellow and red dashed lines indicate the radar azimuth range over the region of interest. In the Fig. 3(b), KDAX radar azimuth ranges from 255 to 330°. The KDAX radar beam at 1.45° tilt is occluded between 260 and 290° and

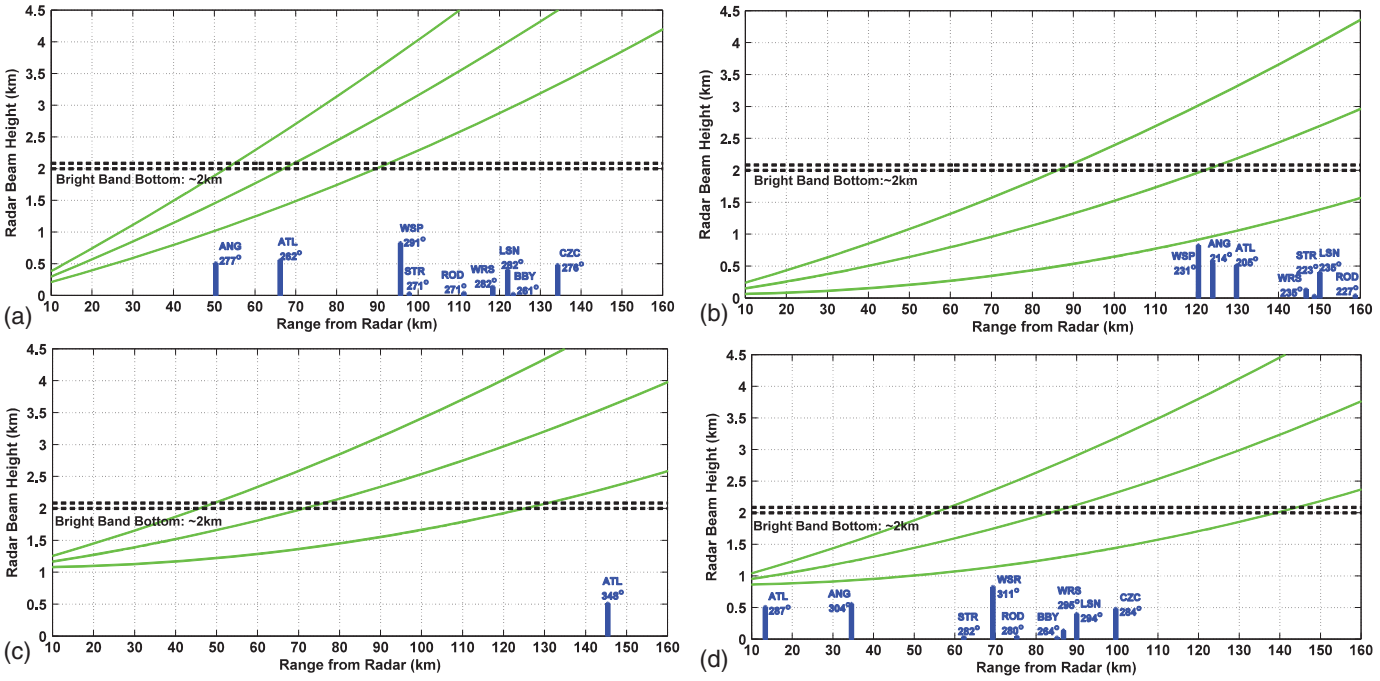

Fig. 2. (Color) Beam heights: (a) 1.45° sweep of KDAX radar; (b) 0.5° sweep of KBBX radar; (c) 0.5° sweep of KMUX radar; (d) 0.5° sweep of KPIX radar, where the green lines are beam top, center, and bottom; blue bars show heights of validation gauges above MSL, and range and azimuth relative to radars; black dashed lines indicate sample bright band height for rainfall event March 14, 2014

is highlighted by the light blue region in the Fig. 3(a). The Fig. 3(c) shows that there is no beam blockage for KPIX at 0.0 degree as it scans in azimuth from 260 to 340°, where the beam bottom is again the red horizontal line. The red crosses in the middle and bottom panel indicate relative direction in azimuth and height of validation gauges in regard to the radar position.

Evaluation

Comparison of QPEs is performed on a pixel-by-pixel manner. The MRMS QPE products are output onto a gridded map in 0.01° latitude and longitude resolution, which is approximately 1.11 km N-S and 0.87 km E-W. Accumulations from the validation gauges are interpolated to the same grids to facilitate comparisons between the gauge amounts and the MRMS-derived QPE. The validation gauge QPE is derived from an inverse distance weighting (IDW) scheme described in Simanton and Osborn (1980), which is defined as follows:

$$F(x,y) = \sum_{i=1}^{n} w_i(x,y) f_i \tag{2}$$

$$w_i(x,y) = \frac{\frac{1}{d_i^b}}{\sum_{i=1}^{n} \frac{1}{d_i^b}} \tag{3}$$

where f_i = gauge value; b = power parameter; d_i = distance from interpolation point to gauge i; and i = gauge number. In this paper, $b = 2$ and a radius of influence is used such that the distance for the radius of influence extrapolates the gauge point value over the approximate area of a single radar pixel and provides a more representative comparison between various QPE products and validation gauge measurements.

In addition to the MRMS QPE products, evaluation is also performed for a Simple KPIX rainfall product. In order to derive Simple KPIX QPE, the KPIX radar reflectivity measurements are gridded to a 0.01° latitude-longitude grids covering the domain of interest accounting for the Earth's curvature. The rainfall rates are then calculated using the Martner $Z - R$ relation given in Eq. (1). Rainfall amounts at different time scales can then be obtained by accumulating rainfall rates from each consecutive scan that typically occurs every minute. This QPE technique determines rainfall rate only from radar reflectivity and no rain gauge data is used. Therefore, it has the advantage of avoiding the complexity involved in generating QPE in the MRMS system. During the rainfall events in this study, the majority of KPIX radar scans are conducted at an elevation angle of 0.5° with a few at 0.0°. For simplicity, only 0.5° elevation measurements are used to derive non-MRMS, KPIX-only QPE.

Statistics of interest for this study include the root-mean-square-error (RMSE), normalized mean bias (NB), correlation coefficient (CC), and the normalized standard error (NSE), which are calculated by comparing the common grid points between the MRMS QPE fields and the validation gauge QPE fields as follows:

$$\text{RMSE} = \sqrt{(R_R - R_G)^2} \tag{4}$$

$$\text{NB} = \frac{\langle R_R - R_G \rangle}{\langle R_G \rangle} \tag{5}$$

$$\text{CC} = \frac{\sum[(R_R - \langle R_R \rangle)(R_G - \langle R_G \rangle)]}{\sqrt{\sum (R_R - \langle R_R \rangle)^2} \sqrt{\sum (R_G - \langle R_G \rangle)^2}} \tag{6}$$

$$\text{NSE} = \frac{\langle |R_R - R_G| \rangle}{\langle R_G \rangle} \tag{7}$$

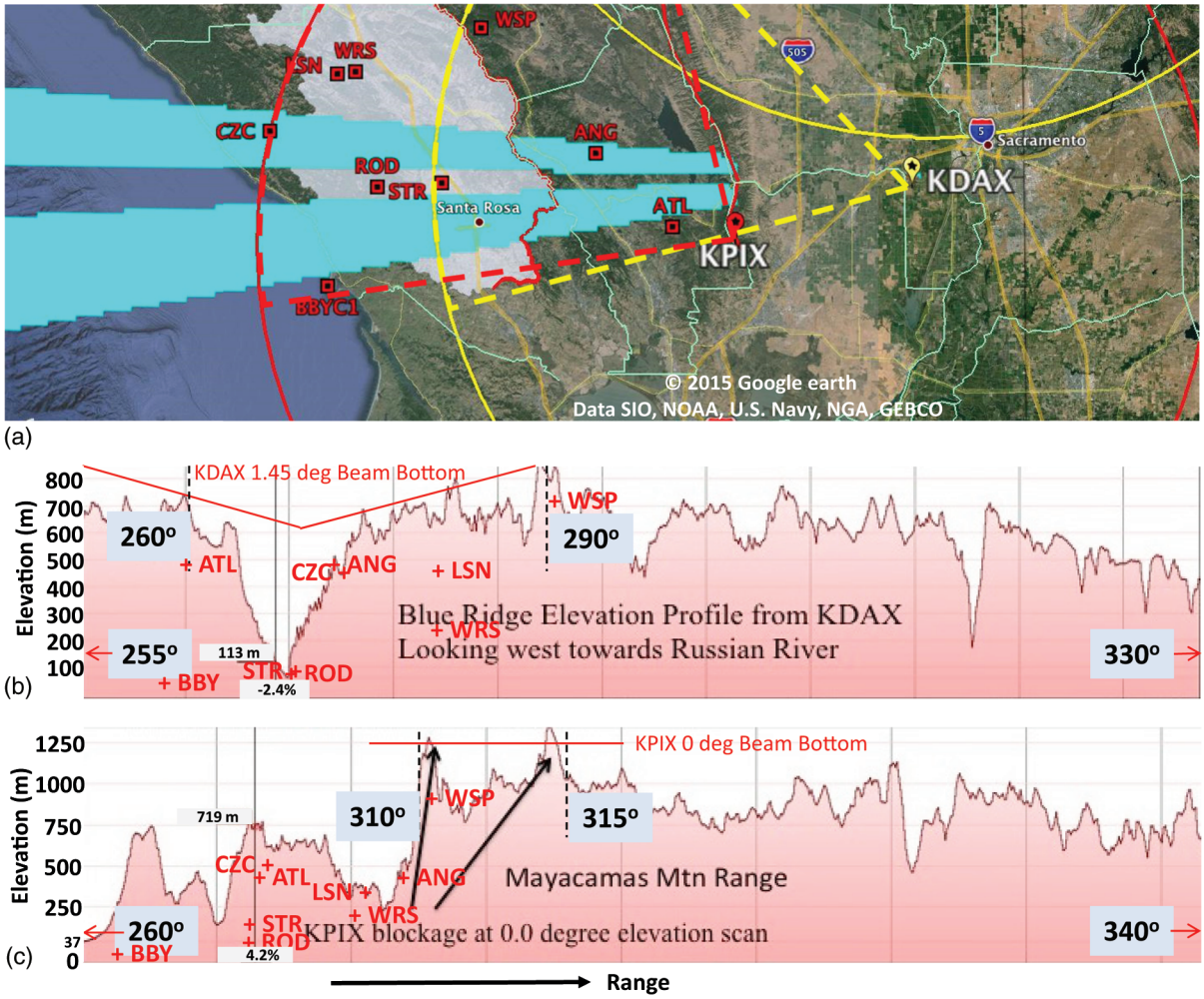

Fig. 3. (Color) (a) Mountain profiles of beam blockage for KDAX and KPIX radar in the direction of the Russian River basin (Data SIO, NOAA, U.S. Navy, NGA, GEBCO, Image Landsat © 2015 Google, Data LDEO-Columbia, NSF, NOAA); (b) KDAX radar beam at 1.45° tilt is blocked between 260 and 290°; (c) red horizontal line is KPIX radar 0.0° beam bottom, indicating no beam blockage

where R_R = QPE estimate; R_G = validation gauge measurement; and the angle brackets indicate the sample average.

In order to minimize the errors introduced from miniscule rainfall amounts, a threshold criterion was applied to ensure the statistics were representative of consistent rainfall accumulating events. This criteria was derived by comparing the hourly rainfall product values with the hourly validation gauge rainfall values. It has been found that rainfall estimates of 2 mm or below generated *NSE*s much greater than 100%. For illustration purposes, Fig. 4(a) shows the NSEs for MRMS radar-only rainfall product on December 23, 2012, whereas Fig. 4(b) illustrates and NSEs of MRMS radar rainfall products with VPR and gauge correction. Here the errors become smaller with increasing accumulation.

Results and Discussion

The QPE evaluation consists of two components: determine which QPE methodology produces the best QPE in the lower Russian River basin and evaluate the impact of KPIX in this region. An evaluation of KPIX was conducted to quantify the impact of using this radar data for QPE because, as noted previously, the nearest NEXRAD (i.e., KDAX) is severely blocked at low scan elevations (below 1.45°) over the Russian River watershed in Sonoma County, and both KMUX and KBBX NEXRAD are sampling well above the bright band (Fig. 2). As noted previously, KPIX is located on Mt. Vaca (elevation of 860 m MSL) and has an unobstructed view of the precipitation in this area. Assuming KPIX is well calibrated and attenuation at C-band is not severe, it is anticipated that KPIX data would produce the best radar-based QPE for the validation gauges shown in Fig. 1. Vertically pointing S-band profiler (STR) data indicates bright band height near the Russian River watershed. An example is presented in Fig. 5, which shows a time-height section of precipitation over the S-band profiler at Santa Rosa from 00Z on December 21, 2012 through 00Z on December 23, 2012. Fig. 5 also shows the height of the KPIX beam at 0.0 and 0.5° in regards to the bright band observed height, and the NEXRAD radar KDAX beam height at 1.3°.

A visual assessment of low elevation reflectivity scans from KPIX and KDAX is presented in Fig. 6. This example illustrates the ability of KPIX for sensing incoming precipitation across Sonoma County and beam blockage suffered by KDAX.

To further evaluate the impact of KPIX and determine which method of generating QPE is best in a quantitative manner, several different QPE grids, representing radar-only, gauge-only, and combination of radar and gauge correction were generated. The 1, 3, and 6 h comparisons of QPE with the validation gauges for normalized mean bias, normalized standard error, correlation

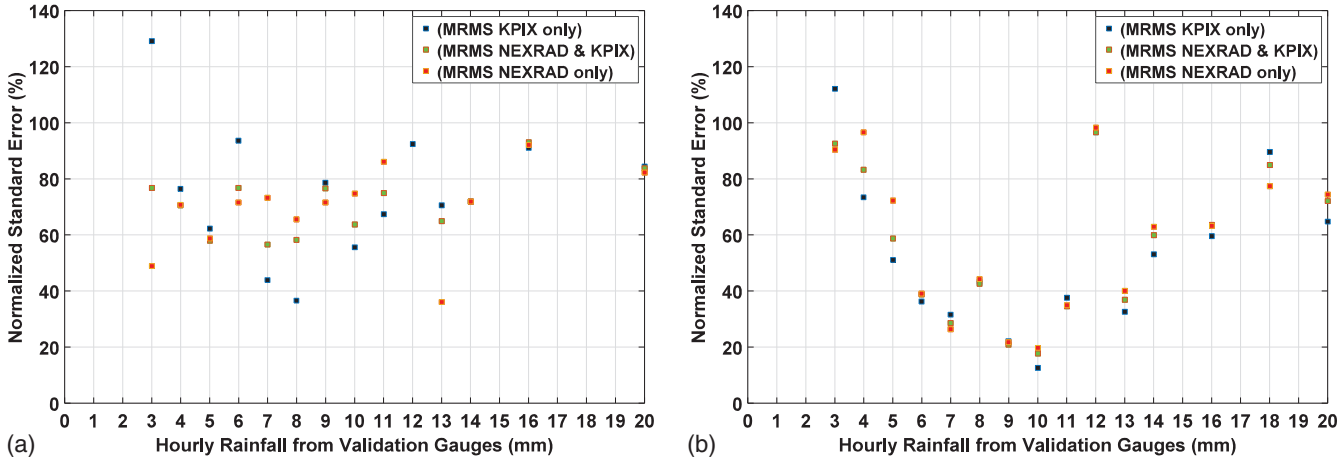

Fig. 4. (Color) Normalized standard error (%) of MRMS QPE products versus validation gauge amounts for 1 h accumulation on December 23, 2012: (a) MRMS radar only product; (b) MRMS radar with VPR and gauge correction product

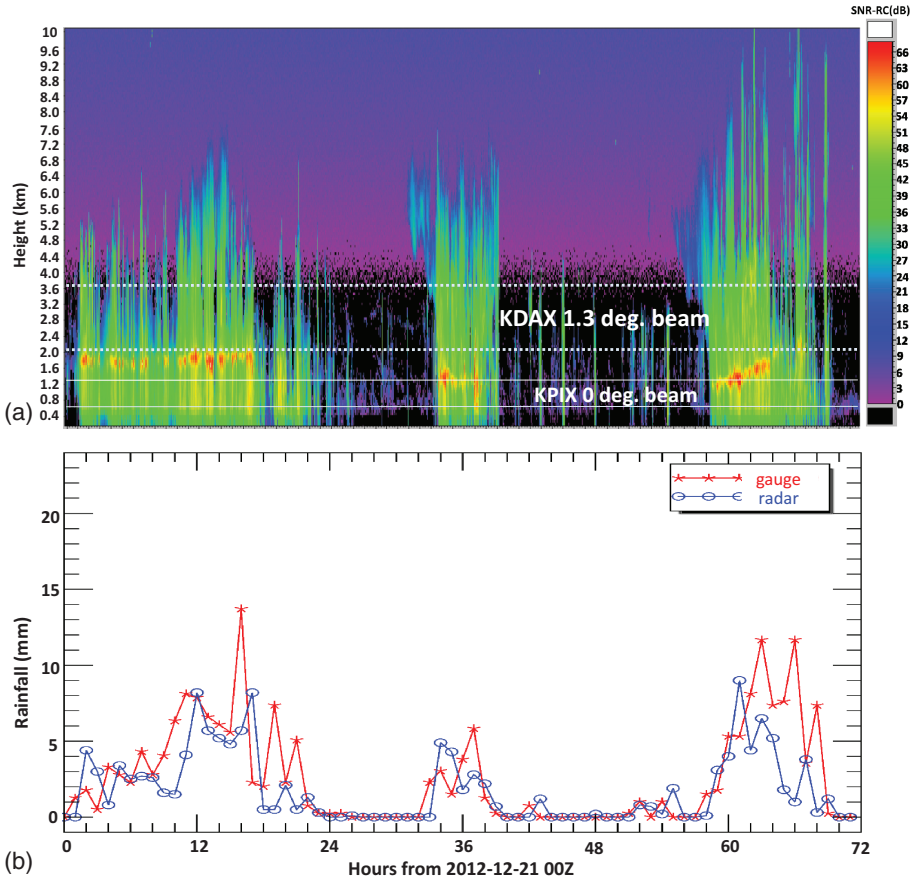

Fig. 5. (Color) (a) Time series of Santa Rosa S-band profiler radar signal-to-noise ratio from 00Z on December 21 to 00Z on December 23, 2012, white dashed lines are KDAX beam width (1.3° tilt) and white solid lines are KPIX beam width (0.0° tilt); (b) corresponding time series of 1 h rain accumulation from gauge located near profiler and MRMS KPIX-only based rainfall estimates

coefficient, and the root mean square error are shown in Fig. 7. The numerical results of all four statistics are also given in Table 2.

The MRMS QPE to the validation gauge comparisons are conditioned on the KPIX beam sampling below the bright band (BB) and the validation gauge observing more than 2 mm of precipitation in a six-hour period where the choice of $Z - R$ is appropriate for nonbright band conditions. The conditioning means that comparisons between QPE products and validation gauges occur only when the top of KPIX beam is below the bright band (Fig. 2) at the location of each validation gauge. It is anticipated that sampling below the BB (i.e., rain region, Fig. 2) provides the biggest impact of KPIX for QPE performance. The primary metrics of measurement are the normalized mean bias and the normalized standard error. This is done to show the percentage differences

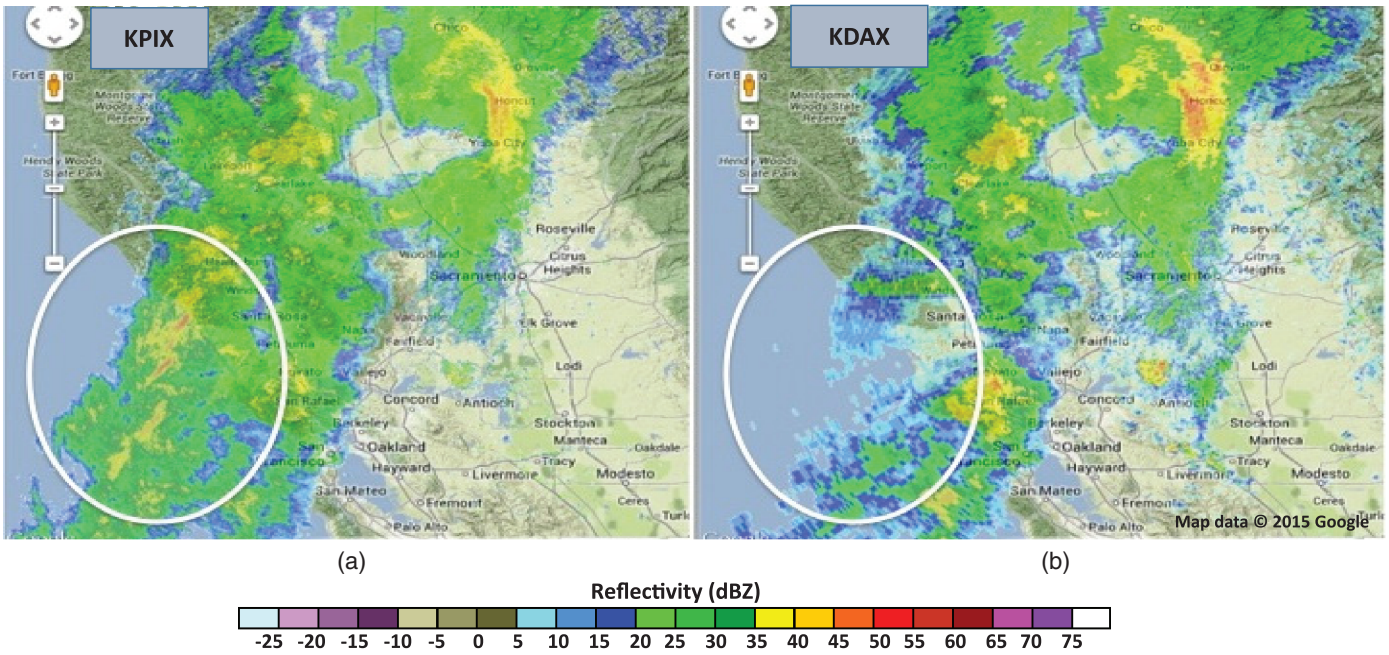

Fig. 6. (Color) Radar reflectivity from (a) KPIX (0.0° tilt); (b) KDAX radar (0.5° tilt) at 14:48Z December 21, 2012; white ellipse shows blockage of KDAX radar beam. (Map data © 2015 Google)

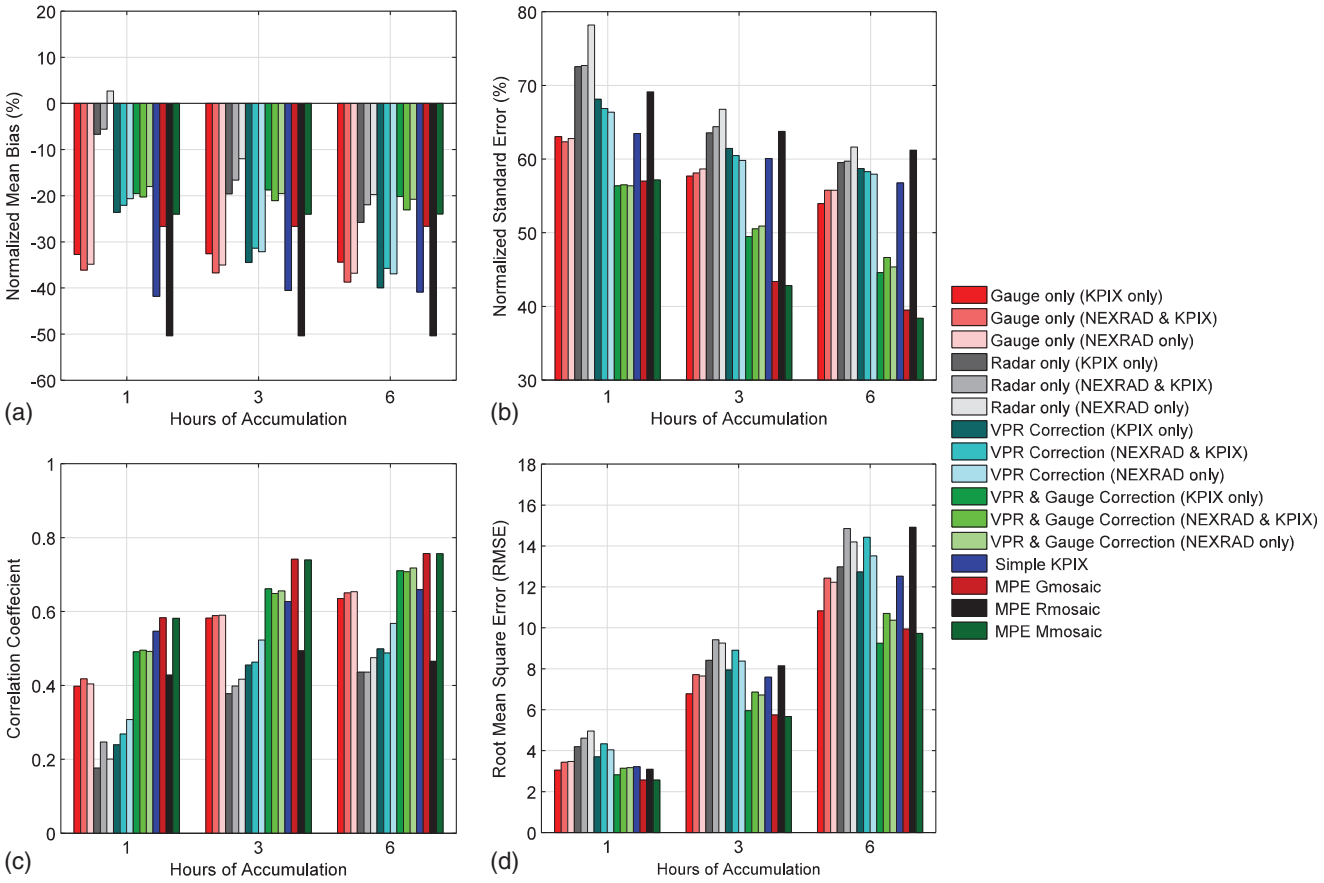

Fig. 7. (Color) Evaluation results of 1, 3, and 6 h rainfall products: (a) normalized mean bias; (b) normalized standard error; (c) correlation coefficient; (d) root mean square error

between the radar and gauge pairs. The additional metrics of correlation coefficient and root mean square error are provided and give additional information regarding the QPE performance. In operating the MRMS code in a retrospective mode, the observed hourly rainfall from the analysis gauges is used to bias correct the radar observations for that hour. Operationally this would not be possible, as not all the gauges report on an hourly basis with rainfall computed at the top of each hour. This provides a significant

Table 2. MRMS QPE Products and Simple KPIX QPE for 1, 3, and 6-h Accumulation Periods

Period of accumulation (h)	MRMS product	MRMS radar input	RMS error (mm)	CC (%)	NB (%)	NSE (%)
1	Gauge only	KPIX only	3.05	40	−32.74	63.06
1	Gauge only	NEXRAD + KPIX	3.43	42	−36.12	62.33
1	Gauge only	NEXRAD only	3.47	40	−34.86	62.78
1	Radar only	KPIX only	4.19	18	−6.70	72.55
1	Radar only	NEXRAD + KPIX	4.61	25	−5.57	72.71
1	Radar only	NEXRAD only	4.96	20	2.68	78.20
1	Radar with VPR	KPIX only	3.70	24	−23.59	68.13
1	Radar with VPR	NEXRAD + KPIX	4.33	27	−22.08	66.87
1	Radar with VPR	NEXRAD only	4.04	31	−20.62	66.36
1	Radar with VPR & GC	KPIX only	2.82	49	−19.52	56.36
1	Radar with VPR & GC	NEXRAD + KPIX	3.14	50	−20.27	56.51
1	Radar with VPR & GC	NEXRAD only	3.17	49	−18.00	56.36
1	Non-MRMS product (simple KPIX QPE)	KPIX only	3.22	55	−41.80	63.47
3	Gauge only	KPIX only	6.77	58	−32.56	57.68
3	Gauge only	NEXRAD + KPIX	7.72	59	−36.70	58.09
3	Gauge only	NEXRAD only	7.65	59	−35.01	58.65
3	Radar only	KPIX only	8.42	38	−19.60	63.55
3	Radar only	NEXRAD + KPIX	9.42	40	−16.62	64.38
3	Radar only	NEXRAD only	9.26	42	−11.98	66.75
3	Radar with VPR	KPIX only	7.94	46	−34.47	61.43
3	Radar with VPR	NEXRAD + KPIX	8.91	46	−31.38	60.48
3	Radar with VPR	NEXRAD only	8.38	52	−32.12	59.83
3	Radar with VPR & GC	KPIX only	5.96	66	−18.72	49.47
3	Radar with VPR & GC	NEXRAD + KPIX	6.87	65	−21.08	50.52
3	Radar with VPR & GC	NEXRAD only	6.72	66	−19.53	50.90
3	Non-MRMS product (simple KPIX QPE)	KPIX only	7.59	63	−40.55	60.08
6	Gauge only	KPIX only	10.83	64	−34.36	53.96
6	Gauge only	NEXRAD + KPIX	12.43	65	−38.70	55.77
6	Gauge only	NEXRAD only	12.22	65	−36.78	55.76
6	Radar only	KPIX only	12.98	44	−25.76	59.54
6	Radar only	NEXRAD + KPIX	14.85	44	−21.93	59.70
6	Radar only	NEXRAD only	14.19	47	−19.76	61.64
6	Radar with VPR	KPIX only	12.73	50	−39.93	58.71
6	Radar with VPR	NEXRAD + KPIX	14.43	49	−35.74	58.30
6	Radar with VPR	NEXRAD only	13.51	57	−36.93	57.95
6	Radar with VPR & GC	KPIX only	9.24	71	−20.16	44.59
6	Radar with VPR & GC	NEXRAD + KPIX	10.70	71	−23.05	46.64
6	Radar with VPR & GC	NEXRAD only	10.37	72	−20.76	45.36
6	Non-MRMS product (simple KPIX QPE)	KPIX only	12.52	66	−40.87	56.77

Note: MRMS products are gauge-only, radar-only, radar with VPR, and radar with VPR and gauge correction.

advantage to the gauge bias correction scheme for MRMS. Fig. 7 also includes the Simple KPIX rainfall evaluation results.

In general, the normalized mean bias [Fig. 7(a)] shows that for below the BB almost all the methods underestimate QPE with respect to the validation gauges for the 1 to 6 h accumulation periods. Fig. 7(a) also indicates that for each MRMS product group (e.g., radar-only QPEs), the biases tend to be within close proximity of one another, which gives the sense that varying radar input doesn't alter the bias significantly. For 1 h accumulations, the MRMS radar-only QPE shows the least amount of bias in comparison to the MRMS QPE with VPR and gauge correction and the MRMS gauge-only products; however, the radar-only also show low correlation [Fig. 7(c)]. An example of the data scatter for 1 h accumulation of the MRMS QPE products and the Simple KPIX QPE is seen in Fig. 8 when driven by KPIX only radar input. The radar-only bias slightly increases (becomes more negative) as the accumulation period increases, and is essentially the same as the VPR and gauge correction QPEs at the 6 h accumulation period. For the other statistics, MRMS radar-only gives the highest error for all products (poorest performance). The Simple KPIX QPE produces the greatest negative bias and is much larger than the MRMS KPIX QPE, but at the same time shows good correlation results.

Initially, VPR correction was not anticipated to impact QPE for locations below the BB. However, in the mean bias results, when considering MRMS radar with VPR correction [Fig. 7(a), Table 2], these show larger bias in regards to the MRMS radar-only, and the normalized standard error is reduced with respect to MRMS radar-only. This indicates that MRMS VPR correction is decreasing the radar-only QPE by some quantity (more bias), such that the overall errors are less with respect to radar-only. The larger bias with VPR correction is most likely attributable to the fact the MRMS software is using the RUC model analysis of freezing level instead of the S-Profiler (STR) observed freezing level where the height used for correction maybe lower than the direct profiler observations. Additional analysis is needed to verify this hypothesis but is beyond the scope of this study.

Considering the normalized standard error for these same products [Fig. 7(b)], the best performance is seen in the MRMS with VPR and gauge correction, and there is very little difference in performance among the products with different radar input. The VPR and gauge correction QPE also performed best in terms of

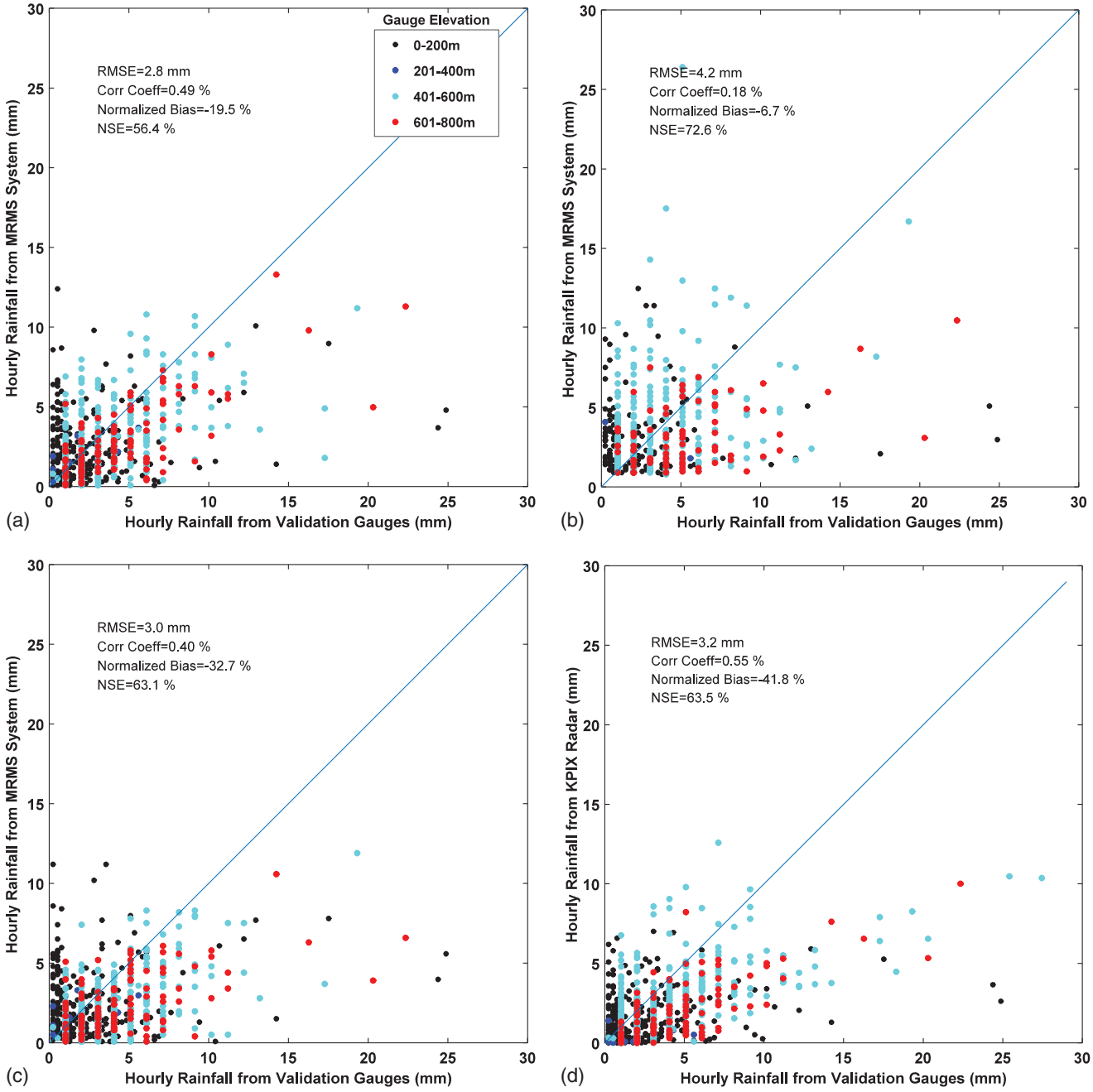

Fig. 8. (Color) Scatter plots of MRMS and simple-KPIX rainfall estimates versus validation gauge observations: (a) MRMS radar-only; (b) MRMS gauge-only; (c) MRMS radar with VPR and gauge correction; (d) KPIX-only; validation gauge elevations are color-coded

correlation coefficient [Fig. 7(c)] and for RMS error [Fig. 7(d)] over the range of accumulation periods.

MRMS gauge-only products provide the second best performance overall. However, these products have a large consistent negative bias in 1, 3, and 6 h accumulation QPE, which is also unanticipated given the location of several analysis gauges in the Russian River basin (Fig. 1). The gauge bias is explored in more detail below. The results for NSE show similar trends to the correlation coefficient and to the root mean square error (Table 2).

In order to understand and interpret the large bias given by the MRMS gauge-only results in reference to the validation gauges [Fig. 7(a), 35–40% negative bias], a non-MRMS gauge bias analysis between the MRMS input gauges and validation gauges (i.e., the green and red gauges in Fig. 1) was conducted. This approach calculates the bias between each individual validation gauge and the surrounding analysis gauges that occur within a specified radius of influence. In Fig. 9, the normalized bias is shown for each validation gauge and the corresponding analysis gauges (color-coded with symbols). The radius of influence is varied from 5 to 40 km. These overall results show good agreement between the gauges. The cumulative bias is indicated by the red dashed line and is within 10% of zero. As mentioned previously, the MRMS gauge-only product goes through a QC process, and is then corrected using radar data (Ware 2005). Therefore, the large biases seen between MRMS gauge-only product may stem from either the QC process or the radar correction technique.

MPE was also used to contrast the performance of the MRMS QPE on a subset of cases (10 days) when MPE data was available.

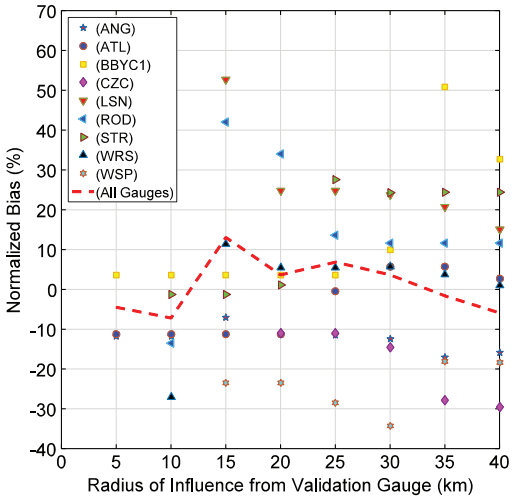

Fig. 9. (Color) Normalized mean bias as a function of radius of influence from validation gauges

MPE uses a different approach to construct gauge-only and bias adjusted radar QPEs. Specifically, the MPE gauge-only QPE (GMOSAIC) uses PRISM climatology, similar to the Mountain Mapper technique used by the CNRFC. The MPE results are added in Fig. 7 and indicate that the combined radar-gauge MPE product (MMOSAIC) performed similarly and slightly better with a NSE of 57.2%, 42.8%, and 38.4% for 1 h, 3 h, and 6 h, respectively, than GMOSAIC with values of 57.0%, 43.4%, and 39.5% for 1 h, 3 h, and 6 h, respectively, further pointing to the challenge of using radar data for QPE in the Russian River basin.

Conclusions

The evaluation results of different rainfall products for the coastal rainfall events in this study indicate that the MRMS QPE product that implements VPR and gauge correction gives the best overall performance. Except for the bias, the non-MRMS Simple KPIX radar-only QPE does as good as the MRMS radar-only QPE products where the large bias can be attributed to KPIX calibration and attenuation. Results from varying the MRMS radar input on the QPE products indicate that there is not much difference in performance between KPIX and NEXRAD, such that the use of KPIX only radar input is equivalent to driving MRMS with NEXRAD only radar-input. Conceptually, the combination of KPIX and NEXRAD would provide the best combination of input data and would be thought to perform best overall. Nevertheless, the errors attributable to the complex terrain gradient may outweigh this advantage. QPE using KPIX can be compromised because of the manner in which the radar is calibrated, where the amount of calibration, clutter filtering, and scan strategies have not been formalized. However, the use of KPIX does informally provide operational forecasters within the local forecast office with improved situational awareness (i.e., a heads-up on storms moving into the area), which NEXRAD cannot provide for this particular region.

In regards to real-time QPE calculation, gauge correction to improve QPE is not possible. For these kinds of requirements, the MRMS product radar with VPR correction shows good performance without the use of gauge correction. Simple KPIX for this type of application does show good correlation but has large bias. Without the availability of gauge data for real-time applications, the value of KPIX becomes more important for forecasters in order to better observe incoming precipitation and assess flash flood potential at short time intervals (one hour or less).

Acknowledgments

This research was supported by the Sonoma County Water Agency and the NOAA OAR Physical Sciences Division. The authors are grateful for computer support from staff at the National Severe Storm Laboratory, and to the three anonymous reviewers for their insightful comments.

References

Benjamin, S. G., et al. (2004). "An hourly assimilation-forecast cycle: The RUC." *Mon. Weather Rev.*, 132(2), 495–518.

Bringi, V. N., and Chandrasekar, V. (2001). *Polarimetric Doppler weather radar: Principles and applications*, Cambridge University Press, New York.

Chen, H., and Chandrasekar, V. (2015). "The quantitative precipitation estimation system for Dallas–Fort Worth (DFW) urban remote sensing network." *J. Hydrol.*, 531(2), 259–271.

Cifelli, R., and Chandrasekar, V. (2010). "Dual polarization radar rainfall estimation." *Rainfall: State of the science*, F. Y. Testik and M. Gebremichael, eds., American Geophysical Union, Washington, DC, 105–125.

Cifelli, R., Chen, H., Willie, D., Reynolds, D., Campbell, C., and Sukovich, E. (2013). "Uncertainty analysis of radar and gauge rainfall estimates in the Russian river basin." *American Geophysical Union (AGU) Fall Meeting*, American Geophysical Union (AGU), Washington, DC.

Fulton, R., Breidenbach, J., Seo, D.-J., Miller, D., and O'Bannon, T. (1998). "The WSR-88D rainfall algorithm." *Weather Forecasting*, 13(2), 377–395.

Kitchen, M., Brown, R., and Davies, A. G. (1994). "Real-time correction of weather radar data for the effects of bright band, range and orographic growth in widespread precipitation." *Q. J. Roy. Meteorol. Soc.*, 120(519), 1231–1254.

Kitzmiller, D., et al. (2011). "Evolving multisensor precipitation estimation methods: Their impacts on flow prediction using a distributed hydrologic model." *J. Hydrometeor*, 12(6), 1414–1431.

Lawrence, B., Shebsovich, M., Glaudemans, M., and Tilles, P. (2003). "Enhancing precipitation estimation capabilities at National Weather Service field offices using multisensor precipitation data mosaics." *Proc., 19th Conf. on Interactive Information Processing Systems*, American Meteorological Society, Boston.

Maddox, R., Zhang, J., Gourley, J., and Howard, K. (2002). "Weather radar coverage over the contiguous United States." *Weather Forecasting*, 17(4), 927–934.

Martner, B. E., Yuter, S. E., White, A. B., Matrosov, S. Y., Kingsmill, D. E., and Ralph, F. M. (2008). "Raindrop size distributions and rain characteristics in California coastal rainfall for periods with and without a radar bright band." *J. Hydrometeorol.*, 9(3), 408–425.

Matrosov, S. Y., Ralph, F. M., Neiman, P. J., and White, A. B. (2014). "Quantitative assessment of operational weather radar rainfall estimates over California's northern Sonoma county using HMT-West data." *J. Hydrometeorol.*, 15(1), 393–410.

Ralph, M. F., Neiman, P. J., Kiladis, G. N., Weickmann, K., and Reynolds, D. W. (2011). "A multiscale observational case study of a pacific atmospheric river exhibiting tropical-extratropical connections and a mesoscale frontal wave." *Mon. Weather Rev.*, 139(4), 1169–1189.

Schaake, J., Henkel, A., and Cong, S. (2004). "Application of the PRISM climatologies for hydrologic modeling and forecasting in the western U.S." *AMS Conf. on Hydrology*, American Meteorological Society, Boston.

Seo, D. J., Seed, A., and Delrieu, G. (2010). "Radar and multisensor rainfall estimation for hydrologic applications." *Rainfall: State of the Science, Geophysical Monograph Series*, F. Y. Testik and M. Gebremichael, eds., Vol. 191, AGU, Washington, DC, 79–104.

Simanton, J. R., and Osborn, H. B. (1980). "Reciprocal distance estimate of point rainfall." *J. Hydraul. Div. Am. Soc. Civ. Eng.*, 106, 1242–1246.

Vasiloff, S. V., et al. (2007). "Improving qpe and very short term qpf: An initiative for a community-wide integrated approach." *Bull. Am. Meteorol. Soc.*, 88(12), 1899–1911.

Vignal, B., Gall, G., Joss, J., and Germann, U. (2000). "Three methods to determine profiles of reflectivity from volumetric radar data to correct precipitation estimates." *J. Appl. Meteorol.*, 39(10), 1715–1726.

Ware, E. C. (2005). "Corrections to radar-estimated precipitation using observed rain gauge data." Masters thesis, Cornell Univ., Ithaca, NY.

Willie, D., Chen, H., Chandrasekar, V., Cifelli, R., Campbell, C., and Reynolds, D. (2013). "Evaluation of multisensor quantitative precipitation estimation methodologies." *IEEE Int. Geoscience and Remote Sensing Symp. (IGARSS)*, Melbourne, Australia, IEEE, New York, 7.

Zhang, J., et al. (2011a). "National mosaic and multi-sensor QPE (NMQ) system: Description, results, and future plans." *Bull. Am. Meteorol. Soc.*, 92(10), 1321–1338.

Zhang, J., Langston, C., and Howard, K. (2008). "Brightband identification based on vertical profiles of reflectivity from the WSR-88D." *J. Atmos. Oceanic. Technol.*, 25(10), 1859–1872.

Zhang, J., Qi, Y., Kingsmill, D., and Howard, K. (2012). "Radar-based quantitative precipitation estimation for the cool season in complex terrain: Case studies from the NOAA hydrometeorology testbed." *J. Hydrometeorol.*, 13(6), 1836–1854.

Zhang, Y., Reed, S., and Kitzmiller, D. (2011b). "Effects of retrospective gauge-based readjustment of multisensor precipitation estimates on hydrologic simulations." *J. Hydrometeorol.*, 12(3), 429–443.